Localization Based on Channel Impulse Response Estimates

Zehao Yu, *Student Member, IEEE*, Zhenyu Liu, *Student Member, IEEE*, Florian Meyer, *Member, IEEE*, Andrea Conti, *Senior Member, IEEE*, and Moe Z. Win, *Fellow, IEEE*

***Abstract*—Location-awareness using wireless signals is a key enabler for numerous emerging applications. Inspired by the recently proposed soft information (SI)-based localization, this paper develops a localization algorithm based on estimates of the channel impulse response (CIR), which inherently contains position information. We propose a delay-origin uncertainty model for describing the conditional distribution of the delays in CIR given node positions. A scalable localization algorithm is designed using belief propagation (BP) on a factor graph that incorporates the uncertainty model. The performance of the developed algorithm is quantified for mmWave signals using QuaDriGa channel simulator, showing decimeter-level localization accuracy in typical indoor environments.**

***Index Terms*—Localization, soft information, channel impulse response, belief propagation, wireless networks.**

I. Introduction

Location-aware networks [1]–[6] are essential for several emerging applications such as crowdsensing [7], autonomous driving [8], environmental monitoring [9], Internet-of-Things (IoT) [10], and big data analysis [11]. A global navigation satellite system (GNSS) is usually used for outdoor scenarios to provide meter-level localization accuracy. In GNSS-challenged environments (e.g., indoor), extensive research has been carried out to devise localization techniques [12]–[19]. Typical localization systems are based on specific technologies or communication systems including Wi-Fi [20]–[25], Bluetooth [26]–[29], ultra-wideband (UWB) [30]–[38], and mmWave [39]–[42].

In recent years, design and analysis of location-aware networks that embrace different technologies become increasingly important. For example, next generation wireless networks will integrate IoT, B5G, mmWave, and TeraHertz technologies. Therefore, it is essential to design localization techniques exploiting all available positional information provided by different technologies. These localization techniques should account for the properties of the wireless channels rather than for technology-specific signal features.

The most fundamental description of the channel given the wireless environment and the node positions is the channel impulse response (CIR). The CIR consists of a set of delay-amplitude pairs and represents how a signal propagates from the transmitter to the receiver in the multipath channel. Therefore, we resort to CIR as input to localization algorithms. Note that the CIR can be either measured [43] or estimated from other observations such as channel state information (CSI) measurements [22]–[24]. The natural question is how to fully exploit the information contained in the CIR for the localization purpose.

To address this question, many attempts have been made in range-based localization. Leveraging the fact that ranging using information of line-of-sight (LOS) path is more accurate than using information of non-line-of-sight (NLOS) paths, significant efforts have been put into the task of exploiting the LOS path from CIR estimates for localization. One of the intuitive approaches is to adopt the first delay-amplitude pair of the estimated CIR as the LOS path and perform localization [23]. While this method is easy to implement in practice, its performance is limited since the estimation of the CIR is harmed by the measurement noise or inference error. Furthermore, other mehtods to identify the LOS path are available [44]–[47].

Different from making hard decisions on which CIR component corresponds to the LOS path, the idea of soft information (SI) for localization [48]–[51] has been proposed in recent years. It directly exploits the function of the measurements and positions, which encapsulates all the positional information contained in the measurements. However, a detailed probabilistic model that describes the relationship between the CIR and the positional information is still lacking.

This paper proposes a SI-based localization algorithm that fully exploits the information contained in the CIR, hereafter referred to as CIR-based localization algorithm. First, we propose a delay-origin uncertainty model, which describes the conditional distribution of the delays in CIR given node positions. The model provides a factor graph that describes the location inference problem. Then, we develop a scalable localization algorithm based on belief propagation (BP) technique. As a case study, the performance of the proposed algorithm is quantified for mmWave signals using QuaDriGa [52] channel simulator.

The remaining sections are organized as follows. Section II describes the system model, and Section III presents the

This research was supported in part by the U.S. Department of Commerce, National Institute of Standards and Technology, under Grant 70NANB17H177, and in part by the European Union's Horizon 2020 research and innovation programme under Grant 871249. (*Corresponding author: M. Z. Win.*)

Z. Yu and Z. Liu are with the Wireless Information and Network Sciences Laboratory, Massachusetts Institute of Technology, Cambridge, MA 02139 USA (e-mail: zehaoyu@mit.edu; zliu14@mit.edu).

F. Meyer was with the Wireless Information and Network Sciences Laboratory, Massachusetts Institute of Technology, Cambridge, MA 02139 USA. He is now with the Scripps Institution of Oceanography and the Department of Electrical and Computer Engineering, University of California San Diego, La Jolla, CA, USA (e-mail: flmeyer@ucsd.edu).

A. Conti is with the Department of Engineering and CNIT, University of Ferrara, 44122 Ferrara, Italy (e-mail: a.conti@ieee.org).

M. Z. Win is with the Laboratory for Information and Decision Systems, Massachusetts Institute of Technology, Cambridge, MA 02139 USA (e-mail: moewin@mit.edu).

978-1-7281-0244-3/20/$31.00 ©2020 IEEE

inference technique based on the proposed model. Section IV presents the implementation of the proposed CIR-based localization algorithm. Simulation results are presented in Section V. Finally, Section VI concludes the paper.

Notation: Random variables are displayed in sans serif, upright fonts; their realizations in serif, italic fonts. Vectors are denoted by bold lowercase. For example, a random variable and its realization are denoted by x and x; a random vector and its realization are denoted by $\mathbf{x}$ and $\boldsymbol{x}$. Furthermore, $\|\boldsymbol{x}\|$ and $\boldsymbol{x}^{\mathrm{T}}$ denote the Euclidean norm, the transpose of vector $\boldsymbol{x}$, respectively; $\propto$ indicates equality up to a normalization factor; $f(\boldsymbol{x})$ denotes the probability density function (PDF) of random vector $\mathbf{x}$ (this is a short notation for $f_{\mathbf{x}}(\boldsymbol{x})$); $f(\boldsymbol{x}|\boldsymbol{y})$ denotes the conditional PDF of random vector $\mathbf{x}$ conditioned on random vector $\mathbf{y}$; $p(\boldsymbol{x})$ denotes the probability mass function (PMF) of discrete random vector $\mathbf{x}$. Operator $\mathbb{P}\{\cdot\}$ denotes the probability of the argument. $\delta(\cdot)$ represents the Dirac Delta function.

II. System Model

Consider a localization network consisting of one agent and N anchors, where the agent represents a device with unknown position while an anchor represents a device with known position. Let $\mathbf{p}_{\mathrm{a}} \in \mathbb{R}^2$ and $\mathbf{p}_i \in \mathbb{R}^2,\ i = 1, 2, \ldots, N$ denote the positions of agent and anchors, respectively.[1] The anchors are at known positions, thus

$$f(\boldsymbol{p}_i) = \delta(\boldsymbol{p}_i - \boldsymbol{p}_i^{\mathrm{c}}), \quad i = 1, 2, \ldots, N \tag{1}$$

where $\boldsymbol{p}_i^{\mathrm{c}}$ denotes the position of anchor i which is constant.[2] The prior of the agent's position, $f(\boldsymbol{p}_{\mathrm{a}})$, is set to be uniform. Consider that all the positions are mutually independent, i.e., the prior distribution of $\mathbf{p} = \left[\mathbf{p}_1^{\mathrm{T}}\ \mathbf{p}_2^{\mathrm{T}} \ldots \mathbf{p}_N^{\mathrm{T}}\ \mathbf{p}_{\mathrm{a}}^{\mathrm{T}}\right]^{\mathrm{T}}$ is

$$f(\boldsymbol{p}) = f(\boldsymbol{p}_{\mathrm{a}}) \prod_{i=1}^{N} f(\boldsymbol{p}_i). \tag{2}$$

In order to perform localization, the agent communicates with all the N anchors, and collects a set of CIR measurements with respect to each anchor. Our goal is to estimate the position of the agent $\mathbf{p}_{\mathrm{a}}$ based on the collected CIR measurements or estimates. Section II-A to II-C describe this procedure in detail.

A. CIR Measurement Model

We consider a general CIR measurement model where $\boldsymbol{\tau}_i = \left[\tau_{i1}\ \tau_{i2}\ \ldots\ \tau_{iL_i}\right]^{\mathrm{T}}$ and $\boldsymbol{\alpha}_i = \left[\alpha_{i1}\ \alpha_{i2}\ \ldots\ \alpha_{iL_i}\right]^{\mathrm{T}}$ denote the measurement vectors of the delays and amplitudes of the CIR between the agent and anchor i, respectively. Here, L_i is the number of multipath between the agent and anchor i. By denoting the true delays as $\boldsymbol{\theta}_i = \left[\theta_{i1}\ \theta_{i2}\ \ldots\ \theta_{iL_i}\right]^{\mathrm{T}}$, we model each component of the delay measurements, τ_{ij}, as a Gaussian random variable with mean θ_{ij} and variance σ_{ij}^2. To decide the variance σ_{ij}^2, we consider two different cases: (i) the CIRs are indirectly estimated from other measurements, and σ_{ij} is set to be the corresponding estimation uncertainty of the delays [53], [54]; and (ii) the CIRs are directly measured, and σ_{ij} is set to be inversely proportional to the square of corresponding measured amplitude [35], [55]. For both cases, we further assume that given θ_{ij}, the measured amplitude α_{ij} is uniformly distributed in a given range. As a result, the conditional distribution of τ_{ij} and α_{ij} given θ_{ij} can be written as[3]

$$\begin{aligned} f(\tau_{ij}, \alpha_{ij}|\theta_{ij}) &= f(\alpha_{ij}|\theta_{ij}) f(\tau_{ij}|\alpha_{ij}, \theta_{ij}) \\ &\propto \varphi(\tau_{ij}; \theta_{ij}, \sigma_{ij}^2(\alpha_{ij})) \end{aligned} \tag{3}$$

where $\varphi(\cdot; \theta_{ij}, \sigma_{ij}^2)$ denotes the Gaussian distribution with mean θ_{ij} and variance σ_{ij}^2.

Let $\boldsymbol{\tau} = \left[\boldsymbol{\tau}_1^{\mathrm{T}}\ \boldsymbol{\tau}_2^{\mathrm{T}} \ldots \boldsymbol{\tau}_N^{\mathrm{T}}\right]^{\mathrm{T}}$, $\boldsymbol{\alpha} = \left[\boldsymbol{\alpha}_1^{\mathrm{T}}\ \boldsymbol{\alpha}_2^{\mathrm{T}} \ldots \boldsymbol{\alpha}_N^{\mathrm{T}}\right]^{\mathrm{T}}$, and $\boldsymbol{\theta} = \left[\boldsymbol{\theta}_1^{\mathrm{T}}\ \boldsymbol{\theta}_2^{\mathrm{T}} \ldots \boldsymbol{\theta}_N^{\mathrm{T}}\right]^{\mathrm{T}}$. Assuming the CIRs from the agent to different anchors are independent, and the components of CIR are also independent, the joint conditional distribution can thus be obtained as

$$f(\boldsymbol{\tau}, \boldsymbol{\alpha}|\boldsymbol{\theta}) = \prod_{i=1}^{N} \prod_{j=1}^{L_i} f(\tau_{ij}, \alpha_{ij}|\theta_{ij}). \tag{4}$$

B. Delay-Origin Uncertainty Model

The relation between the delays of CIRs and agent/anchor positions is discussed in this subsection. In particular, we relate the CIR and the position of agent and anchor i by modeling $f(\boldsymbol{\theta}_i|\boldsymbol{p}_{\mathrm{a}}, \boldsymbol{p}_i)$. One difficulty in modeling $f(\boldsymbol{\theta}_i|\boldsymbol{p}_{\mathrm{a}}, \boldsymbol{p}_i)$ is to assign proper origins to the components of the vector $\boldsymbol{\theta}_i$. Inspired by the probabilistic data association approaches [56]–[58], for each anchor i, we define a discrete value random variable a_i, which is called the association variable and indicates the delay component that represents the path in LOS. If no component is in LOS, then $\mathsf{a}_i = 0$.

To model the PDF of a_i, consider two exclusive events: (i) all the delay components are in NLOS, which has probability P_{NL}; and (ii) one of the delay components is in LOS, which has probability $P_{\mathrm{L}} = 1 - P_{\mathrm{NL}}$. We assume that in the event (ii), each component has equal probability to be in LOS. As a result, the PMF of a_i can be written as

$$p(a_i) = \begin{cases} P_{\mathrm{NL}}, & a_i = 0 \\ (1 - P_{\mathrm{NL}})/L_i, & a_i \in \{1,\ 2,\ \ldots,\ L_i\} \\ 0, & \text{otherwise.} \end{cases} \tag{5}$$

Given a_i and assuming all the delays are independent given $\mathbf{p}_{\mathrm{a}}$ and $\mathbf{p}_i$, we have

$$\begin{aligned} &f(\boldsymbol{\theta}_i|\boldsymbol{p}_{\mathrm{a}}, \boldsymbol{p}_i, a_i) \\ &\quad = \begin{cases} \prod_{j=1}^{L_i} f_{\mathrm{NL}}(\theta_{ij}|\boldsymbol{p}_{\mathrm{a}}, \boldsymbol{p}_i), & a_i = 0 \\ f_{\mathrm{L}}(\theta_{ia_i}|\boldsymbol{p}_{\mathrm{a}}, \boldsymbol{p}_i) \prod_{\substack{j=1 \\ j \neq a_i}}^{L_i} f_{\mathrm{NL}}(\theta_{ij}|\boldsymbol{p}_{\mathrm{a}}, \boldsymbol{p}_i), & a_i \neq 0 \end{cases} \end{aligned} \tag{6}$$

[1] We focus on the two-dimensional localization in this paper, but we will show later that the proposed algorithms can be extended to three-dimensional cases easily.

[2] Note that here $\delta(\cdot)$ is a generalized function, and $f(x) = \delta(x - a)$ represents $\mathbb{P}\{x = a\} = 1$.

[3] Note that we will generate the measurement data using a more complicated model when perform simulations in Section V.

where $f_{\mathrm{L}}(\theta_{ia_i}|\boldsymbol{p}_{\mathrm{a}},\boldsymbol{p}_i)$ denotes the PDF of θ_{ia_i} given $\boldsymbol{p}_{\mathrm{a}}$ and $\boldsymbol{p}_i$ when the a_ith component of the CIR corresponds to the LOS path; while $f_{\mathrm{NL}}(\theta_{ij}|\boldsymbol{p}_{\mathrm{a}},\boldsymbol{p}_i)$ denotes the PDF of θ_{ij} given $\boldsymbol{p}_{\mathrm{a}}$ and $\boldsymbol{p}_i$ in NLOS cases.

The PDF $f_{\mathrm{L}}(\theta_{ia_i}|\boldsymbol{p}_{\mathrm{a}},\boldsymbol{p}_i)$ in LOS condition is modeled as

$$f_{\mathrm{L}}(\theta_{ia_i}|\boldsymbol{p}_{\mathrm{a}},\boldsymbol{p}_i)=\delta\Big(\theta_{ia_i}-\frac{\|\boldsymbol{p}_{\mathrm{a}}-\boldsymbol{p}_i\|}{c_0}\Big) \tag{7}$$

where c_0 is the speed of the light. To model the PDF $f_{\mathrm{NL}}(\theta_{id}|\boldsymbol{p}_{\mathrm{a}},\boldsymbol{p}_i)$, the following two sources that may result in an CIR component being in NLOS are considered: (1) multipath propagation; and (2) erroneously estimated or measured components that are not related to physically existing propagation paths. By introducing a parameter P_{E} which weighs these two sources, we obtain

$$\begin{aligned}&f_{\mathrm{NL}}(\theta_{ij}|\boldsymbol{p}_{\mathrm{a}},\boldsymbol{p}_i)\\&\quad=P_{\mathrm{E}}\,f_{\mathrm{NL,E}}(\theta_{ij})+(1-P_{\mathrm{E}})\,f_{\mathrm{NL,M}}(\theta_{ij}|\boldsymbol{p}_{\mathrm{a}},\boldsymbol{p}_i)\end{aligned} \tag{8}$$

where $f_{\mathrm{NL,M}}(\theta_{ij}|\boldsymbol{p}_{\mathrm{a}},\boldsymbol{p}_i)$ denotes the PDF due to the multipath propagation, and $f_{\mathrm{NL,E}}(\theta_{ij})$ denotes the PDF due to estimation or measuring error. According to [52], [59], we model the PDF of delays of NLOS paths as exponential distribution. Since a NLOS path comes later than the LOS path and earlier than the predefined maximum possible delay $\theta_{\max}$, the $f_{\mathrm{NL,M}}(\theta_{ij}|\boldsymbol{p}_{\mathrm{a}},\boldsymbol{p}_i)$ is modeled as a truncated exponential distribution:

$$\begin{aligned}&f_{\mathrm{NL,M}}(\theta_{ij}|\boldsymbol{p}_{\mathrm{a}},\boldsymbol{p}_i)\\&=\begin{cases}\frac{\xi e^{-\xi(\theta_{ij}-\theta_{\min}(\boldsymbol{p}_{\mathrm{a}},\boldsymbol{p}_i))}}{1-e^{-\xi(\theta_{\max}-\theta_{\min}(\boldsymbol{p}_{\mathrm{a}},\boldsymbol{p}_i))}}\,, & \theta_{\min}(\boldsymbol{p}_{\mathrm{a}},\boldsymbol{p}_i)\leqslant\theta_{ij}<\theta_{\max}\\ 0\,, & \text{otherwise}\end{cases}\end{aligned} \tag{9}$$

where $\theta_{\min}(\boldsymbol{p}_{\mathrm{a}},\boldsymbol{p}_i)=\frac{\|\boldsymbol{p}_{\mathrm{a}}-\boldsymbol{p}_i\|}{c_0}$ and ξ is the parameter for the exponential distribution. The value of ξ depends on the specific channel environment considered. The $f_{\mathrm{NL,E}}(\theta_{ij})$ is modeled as a uniform distribution:

$$f_{\mathrm{NL,E}}(\theta_{ij})=\begin{cases}\frac{1}{\theta_{\max}}\,, & 0\leqslant\theta_{ij}<\theta_{\max}\\ 0\,, & \text{otherwise}\,.\end{cases} \tag{10}$$

The conditional PDF $f(\boldsymbol{\theta}_i|\boldsymbol{p}_{\mathrm{a}},\boldsymbol{p}_i)$ can be obtained by marginalizing out a_i as

$$f(\boldsymbol{\theta}_i|\boldsymbol{p}_{\mathrm{a}},\boldsymbol{p}_i)=\sum_{a_i=0}^{L_i}f(\boldsymbol{\theta}_i|\boldsymbol{p}_{\mathrm{a}},\boldsymbol{p}_i,a_i)p(a_i|\boldsymbol{p}_{\mathrm{a}},\boldsymbol{p}_i)\,. \tag{11}$$

Consider a_i is independent of $\mathbf{p}_{\mathrm{a}}$ and $\mathbf{p}_i$. Replacing $p(a_i|\boldsymbol{p}_{\mathrm{a}},\boldsymbol{p}_i)$ by $p(a_i)$ given in (5), we have

$$\begin{aligned}f(\boldsymbol{\theta}_i|\boldsymbol{p}_{\mathrm{a}},\boldsymbol{p}_i)&=P_{\mathrm{NL}}\prod_{j=1}^{L_i}f_{\mathrm{NL}}(\theta_{ij}|\boldsymbol{p}_{\mathrm{a}},\boldsymbol{p}_i)\\&\quad+\frac{1-P_{\mathrm{NL}}}{L_i}\sum_{a_i=1}^{L_i}f_{\mathrm{L}}(\theta_{ia_i}|\boldsymbol{p}_{\mathrm{a}},\boldsymbol{p}_i)\prod_{\substack{j=1\\j\neq a_i}}^{L_i}f_{\mathrm{NL}}(\theta_{ij}|\boldsymbol{p}_{\mathrm{a}},\boldsymbol{p}_i)\,.\end{aligned} \tag{12}$$

Finally, consider the CIRs of different agent-anchor pairs are independent. From (12), we thus obtain the expression for the joint likelihood function as

$$f(\boldsymbol{\theta}|\boldsymbol{p})=\prod_{i=1}^{N}f(\boldsymbol{\theta}_i|\boldsymbol{p}_{\mathrm{a}},\boldsymbol{p}_i)\,. \tag{13}$$

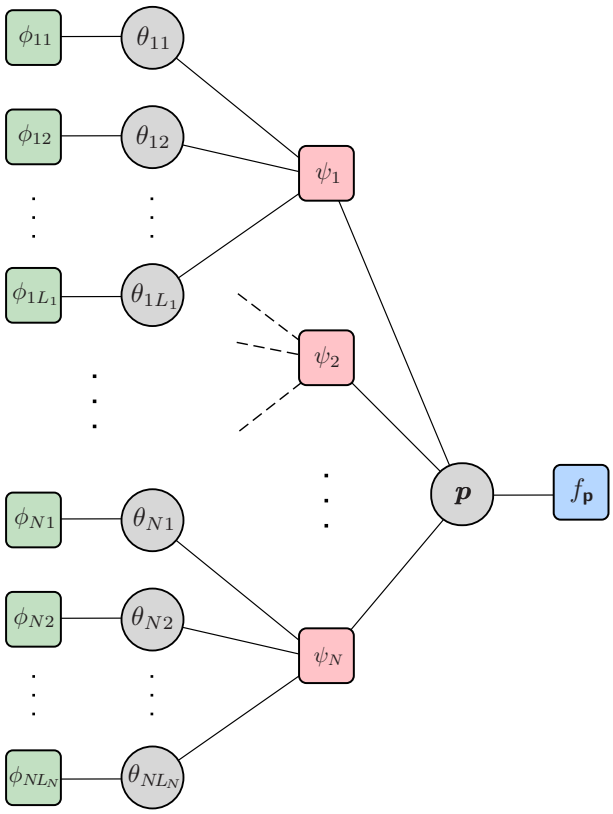

Fig. 1. Factor graph representation of the probabilistic model. For simplicity, we denote the factor nodes with distribution $f_{\boldsymbol{\tau}_{ij},\boldsymbol{\alpha}_{ij}|\boldsymbol{\theta}_{ij}}$ and $f_{\boldsymbol{\theta}_i|\mathbf{p}_{\mathrm{a}},\mathbf{p}_i}$ as ϕ_{ij} and ψ_i, respectively.

C. Graphical Model

Following the Bayesian framework, we derive the joint posterior distribution of the positions $\mathbf{p}$ and delays $\boldsymbol{\theta}$ given the measurements $\boldsymbol{\tau}$ and $\boldsymbol{\alpha}$ as

$$\begin{aligned}f(\boldsymbol{p},\boldsymbol{\theta}|\boldsymbol{\tau},\boldsymbol{\alpha})&\propto f(\boldsymbol{\tau},\boldsymbol{\alpha}|\boldsymbol{p},\boldsymbol{\theta})f(\boldsymbol{p},\boldsymbol{\theta})\\&=f(\boldsymbol{\tau},\boldsymbol{\alpha}|\boldsymbol{\theta})f(\boldsymbol{\theta}|\boldsymbol{p})f(\boldsymbol{p})\end{aligned} \tag{14}$$

where, to obtain the last equation, we assume that given $\boldsymbol{\theta}$, the CIR measurement $\boldsymbol{\tau}$ and $\boldsymbol{\alpha}$ are independent of $\mathbf{p}$. Substituting (2), (4), and (13) into (14) gives

$$\begin{aligned}f(\boldsymbol{p},\boldsymbol{\theta}|\boldsymbol{\tau},\boldsymbol{\alpha})&=f(\boldsymbol{p}_{\mathrm{a}})\prod_{i=1}^{N}f(\boldsymbol{p}_i)\\&\quad\times\prod_{i=1}^{N}\Big[f(\boldsymbol{\theta}_i|\boldsymbol{p}_{\mathrm{a}},\boldsymbol{p}_i)\prod_{j=1}^{L_i}f(\tau_{ij},\alpha_{ij}|\theta_{ij})\Big]\,.\end{aligned} \tag{15}$$

The factorization structure of (15) can be represented by a factor graph as exemplified in Fig. 1.

The goal of the CIR-based localization algorithm is to estimate the posterior distribution of $\mathbf{p}_{\mathrm{a}}$ given the measurements $\boldsymbol{\tau}$ and $\boldsymbol{\alpha}$, i.e., $f(\boldsymbol{p}_{\mathrm{a}}|\boldsymbol{\tau},\boldsymbol{\alpha})$, with which different estimation methods can then be applied to infer the position of the agent, such as the minimum mean square error (MMSE) estimation. The estimated position $\hat{\boldsymbol{p}}_{\mathrm{a}}$ under MMSE criterion is given by

$$\hat{\boldsymbol{p}}_{\mathrm{a}}=\int\boldsymbol{p}_{\mathrm{a}}f(\boldsymbol{p}_{\mathrm{a}}|\boldsymbol{\tau},\boldsymbol{\alpha})\,\mathrm{d}\boldsymbol{p}_{\mathrm{a}}\,. \tag{16}$$

However, to obtain $f(\boldsymbol{p}_{\rm a}|\boldsymbol{\tau},\boldsymbol{\alpha})$, one has to marginalize out $\mathbf{p}_{\rm b} \triangleq \left[\mathbf{p}_1^{\rm T}\ \mathbf{p}_2^{\rm T}\ldots\mathbf{p}_N^{\rm T}\right]^{\rm T}$ and $\boldsymbol{\theta}$, which is intractable. To solve this problem, we propose a BP algorithm based on the factor graph in Fig. 1, which will be introduced in Section III.

III. Message-passing on the Factor Graph

The message-passing (MP) [60] is an inference algorithm performed on graphical models [61]. In particular, factor graphs [62], [63] are a type of graphical models that can represent the factorization of a probability distribution. MP algorithms exploit the factorization structure to efficiently calculate marginal PDFs. In addition, MP algorithms are suitable for a distributed implementation since the messages can be exchanged only with nearby nodes.

The MP algorithm aims to find the distribution g^* which minimizes the Kullback-Leibler (KL)-divergence between g and the desired distribution f from a given family $\mathcal{G}$ [60]. Different choices of the family $\mathcal{G}$ result in different MP algorithms. In this paper, we adopt the MP algorithm based on Bethe approximation [64], which is the well-known BP algorithm [65], [66]. We choose the BP algorithm due to the fact that the BP algorithm provides exactly $g^* = f$ if the desired distribution f has a tree structure [66]. As a result, according to the tree structure shown in Fig. 1, the BP algorithm provides us the optimal solution.

In the rest of this section, we calculate the message and belief update equations based on the BP rule. The belief of the positions of the agent and anchors can be calculated as

$$b(\boldsymbol{p}) \propto f(\boldsymbol{p}) \prod_{i=1}^{N} m_{\psi_i\to\mathbf{p}}(\boldsymbol{p}) \tag{17}$$

where $m_{\psi_i\to\mathbf{p}}(\boldsymbol{p})$ is the message sent from ψ_i to $\mathbf{p}$. It can be calculated as

$$m_{\psi_i\to\mathbf{p}}(\boldsymbol{p}) \propto \int f(\boldsymbol{\theta}_i|\boldsymbol{p}_{\rm a},\boldsymbol{p}_i) \prod_{j=1}^{L_i} \varphi(\theta_{ij};\tau_{ij},\sigma_{ij}^2)\,{\rm d}\boldsymbol{\theta}_i \tag{18}$$

where $\varphi(\theta_{ij};\tau_{ij},\sigma_{ij}^2),\ j=1,2,\ldots,L_i$ are the messages (3) sent from the variable nodes $\theta_{i1},\theta_{i2},\ldots,\theta_{iL_i}$ to the factor node ψ_i. Based on $b(\boldsymbol{p})$, the posterior distribution of the position of the agent given measurements $\boldsymbol{\tau}$ and $\boldsymbol{\alpha}$ can then be expressed as

$$f(\boldsymbol{p}_{\rm a}|\boldsymbol{\tau},\boldsymbol{\alpha}) \propto \int b(\boldsymbol{p})\,{\rm d}\boldsymbol{p}_{\rm b}\,. \tag{19}$$

Substituting (1), (2), and (17) into (19), we have

$$f(\boldsymbol{p}_{\rm a}|\boldsymbol{\tau},\boldsymbol{\alpha}) \propto f(\boldsymbol{p}_{\rm a}) \prod_{i=1}^{N} m_{\psi_i}(\boldsymbol{p}_{\rm a};\boldsymbol{p}_i^{\rm c}) \tag{20}$$

where

$$m_{\psi_i}(\boldsymbol{p}_{\rm a};\boldsymbol{p}_i^{\rm c}) = \int f(\boldsymbol{\theta}_i|\boldsymbol{p}_{\rm a},\boldsymbol{p}_i^{\rm c}) \prod_{j=1}^{L_i} \varphi(\theta_{ij};\tau_{ij},\sigma_{ij}^2)\,{\rm d}\boldsymbol{\theta}_i\,. \tag{21}$$

The notation $f(\boldsymbol{\theta}_i|\boldsymbol{p}_{\rm a},\boldsymbol{p}_i^{\rm c})$ represents the PDF defined in (12) evaluated at $\mathbf{p}_i = \boldsymbol{p}_i^{\rm c}$, i.e., $f_{\boldsymbol{\theta}_i|\mathbf{p}_{\rm a},\mathbf{p}_i}(\boldsymbol{\theta}_i|\boldsymbol{p}_{\rm a},\boldsymbol{p}_i^{\rm c})$.

The structure of (12) makes it possible to perform the integrations in (21) separately. In particular, for LOS components we have

$$\begin{aligned}\int & f_{\rm L}(\theta_{ij}|\boldsymbol{p}_{\rm a},\boldsymbol{p}_i^{\rm c})\,\varphi\big(\theta_{ij};\tau_{ij},\sigma_{ij}^2\big)\,{\rm d}\theta_{ij}\\ &= \varphi\Big(\frac{\|\boldsymbol{p}_{\rm a}-\boldsymbol{p}_i^{\rm c}\|}{c_0};\tau_{ij},\sigma_{ij}^2\Big)\\ &\triangleq m_{ij}^{\rm L}(\boldsymbol{p}_{\rm a})\end{aligned} \tag{22}$$

whereas for NLOS components we have

$$\begin{aligned}&\int f_{\rm NL}(\theta_{ij}|\boldsymbol{p}_{\rm a},\boldsymbol{p}_i^{\rm c})\varphi\big(\theta_{ij};\tau_{ij},\sigma_{ij}^2\big)\,{\rm d}\theta_{ij}\\ &= \frac{P_{\rm E}}{\theta_{\max}}\left[Q\Big(\frac{-\tau_{ij}}{\sigma_{ij}}\Big)-Q\Big(\frac{\theta_{\max}-\tau_{ij}}{\sigma_{ij}}\Big)\right]\\ &\quad+\frac{(1-P_{\rm E})\,\xi\,e^{\xi\theta_{\min}-\xi\tau_{ij}+\frac{1}{2}\xi^2\sigma_{ij}^2}}{1-e^{-\xi(\theta_{\max}-\theta_{\min})}}\\ &\quad\times\left[Q\left(\frac{\theta_{\min}-\tau_{ij}+\xi\sigma_{ij}^2}{\sigma_{ij}}\right)-Q\left(\frac{\theta_{\max}-\tau_{ij}+\xi\sigma_{ij}^2}{\sigma_{ij}}\right)\right]\\ &\triangleq m_{ij}^{\rm NL}(\boldsymbol{p}_{\rm a})\end{aligned} \tag{23}$$

where $Q(\cdot)$ is the Gaussian Q-function of the standard Gaussian distribution, and we denote $\theta_{\min}(\boldsymbol{p}_{\rm a},\boldsymbol{p}_i)$ as $\theta_{\min}$ for simplicity. From (12), (22), and (23), equation (21) can be expressed as

$$\begin{aligned}m_{\psi_i}(\boldsymbol{p}_{\rm a};\boldsymbol{p}_i^{\rm c}) \propto\ & P_{\rm NL}\prod_{j=1}^{L_i} m_{ij}^{\rm NL}(\boldsymbol{p}_{\rm a})\\ &+\frac{1-P_{\rm NL}}{L_i}\sum_{a_i=1}^{L_i} m_{ia_i}^{\rm L}(\boldsymbol{p}_{\rm a})\prod_{\substack{j=1\\ j\neq a_i}}^{L_i} m_{ij}^{\rm NL}(\boldsymbol{p}_{\rm a})\,.\end{aligned} \tag{24}$$

Based on the message update equations (24), the posterior distribution of the position of the agent given measurements $\boldsymbol{\tau}$ and $\boldsymbol{\alpha}$ can then be calculated according to (20).

IV. CIR-based Localization Algorithm

In this section, we first design an efficient method to implement the message update procedure. Then, we present the proposed CIR-based localization algorithm.

Due to the complicated structure of $m_{\psi_i}(\boldsymbol{p}_{\rm a};\boldsymbol{p}_i^{\rm c})$ in (24), direct calculation of the integral in (16) is computationally infeasible. Therefore, we resort to the method of importance sampling [67], which is an efficient approach to perform Monte Carlo integration [68].

The efficiency of importance sampling depends on the proposal distribution from which samples are drawn [67]. Specifically, the algorithm is more efficient if the proposal distribution is close to the target distribution in the sense of minimizing the variance between the two distributions [69]. We propose a novel proposal distribution, named "Gaussian mixture rings", which consists of sets of concentric rings where each ring represents a weighted Gaussian distribution. In particular, we exploit the structure of (24) which is a summation of L_i+1 terms. The term before the plus sign corresponds to the case where all the L_i components of the estimated CIR are NLOS, and each of the rest L_i terms under summation corresponds to

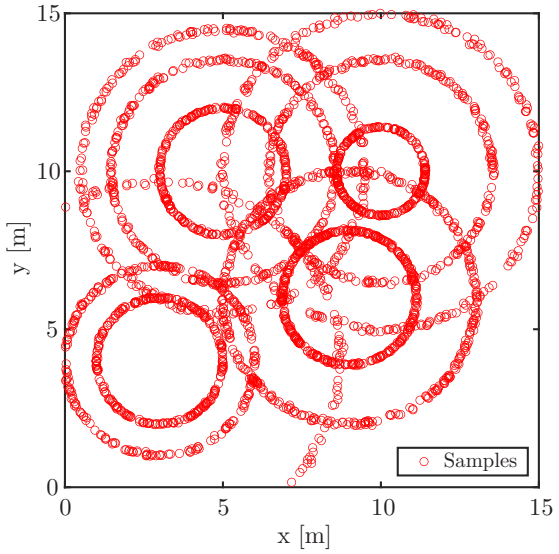

Fig. 2. Samples drawn from the proposal distribution. In particular, in this illustration we consider 1 agent at $(7.5, 7.5)$ m and 4 anchors at $(3, 4)$ m, $(5, 10)$ m, $(9, 6)$ m, and $(10, 10)$ m, respectively.

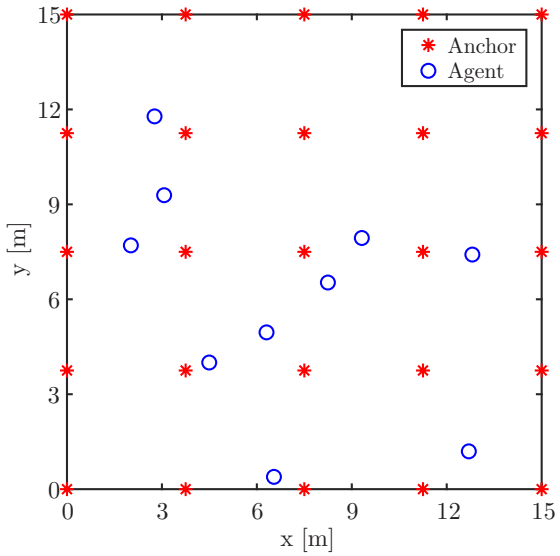

Fig. 3. Layout of anchors and agents.

Algorithm 1 CIR-based Localization Algorithm

Input: The CIR measurements/estimations $\boldsymbol{\tau}$ and $\boldsymbol{\alpha}$;
Output: Inferred positions of the agents $\hat{\boldsymbol{p}}_{\mathrm{a}}$.

1: Initialize the parameters P_{NL}, P_{E}, $\theta_{\max}$, and ξ;
2: **for** $s = 1$ to S **do**
3: Uniformly sample an element i from $\{1, 2, \ldots, N\}$
4: Uniformly sample an element j from $\{1, 2, \ldots, L_i\}$
5: Draw a sample $\tilde{\boldsymbol{p}}_{\mathrm{a}}^{(s)}$ from the Gaussian distribution $\varphi\big(\frac{\|\tilde{\boldsymbol{p}}_{\mathrm{a}}^{(s)} - \boldsymbol{p}_i^{\mathrm{c}}\|}{c_0}; \tau_{ij}, \sigma_{ij}^2\big)$
6: **end for**
7: **for** each sample $\tilde{\boldsymbol{p}}_{\mathrm{a}}^{(s)}$ **do**
8: Calculate the weight $f(\tilde{\boldsymbol{p}}_{\mathrm{a}}^{(s)}|\boldsymbol{\tau}, \boldsymbol{\alpha})/g(\tilde{\boldsymbol{p}}_{\mathrm{a}}^{(s)})$ according to (20) and (25);
9: **end for**
10: Normalize the weights of samples;
11: Perform MMSE estimation on the agent position by calculating the weighted average of the samples;
12: **return** Position estimation of the agent.

the a_ith component of the estimated CIR is LOS. According to (22), $m_{ij}^{\mathrm{L}}(\boldsymbol{p}_{\mathrm{a}})$ is a Gaussian distribution. By approximating the message (23) as uniform, (24) corresponds to a set of rings centered at $\boldsymbol{p}_i^{\mathrm{c}}$ with radius $\tau_{ij} c_0$, $j = 1, 2, \ldots, L_i$. The distribution in (20) is a multiplication of all the messages $m_{\psi_i}(\boldsymbol{p}_{\mathrm{a}}; \boldsymbol{p}_i^{\mathrm{c}})$, $i = 1, 2, \ldots, N$, which are sets of rings centered at $\boldsymbol{p}_i^{\mathrm{c}}, i = 1, 2, \ldots, N$. Based on the structure of (24), we model the proposal distribution as Gaussian mixture rings with the PDF

$$g(\boldsymbol{p}_{\mathrm{a}}) = \frac{1}{N} \sum_{i=1}^{N} \left[\frac{1}{L_i} \sum_{j=1}^{L_i} \varphi\Big(\frac{\|\boldsymbol{p}_{\mathrm{a}} - \boldsymbol{p}_i^{\mathrm{c}}\|}{c_0}; \tau_{ij}, \sigma_{ij}^2 \Big) \right]. \quad (25)$$

An illustration of the proposal distribution (25) is shown in Fig. 2.

Based on the results in Section III and IV, we present the CIR-based localization algorithm in Alg. 1, where S samples are drawn. In particular, this algorithm contains four parts: initialization (Line 1), sample drawing (Lines $2-6$), weight calculation (Lines $7-10$), and MMSE estimation (Line 11). Note that the number of samples S used in the importance sampling determines a trade-off between accuracy and efficiency: a larger number of samples can improve the accuracy, at the price of longer running time.

V. Simulation Results

To validate the proposed algorithm, we perform simulations using QUAsi Deterministic RadIo channel GenerAtor (QuaDRiGa) [52], which generates standardized radio channel impulse responses for system-level simulations of mobile radio networks. Besides its capability of generating realistic channel models, another advantage of QuaDRiGa is that it takes into account the spatial consistency of wireless channels among the nodes.

A. Simulation Settings

We evaluate the proposed algorithm using mmWave system as a case study. In particular, we consider typical indoor office scenarios given by the 3GPP TR 38.901 standard [59] using mmWave signals in the 28 GHz band [70]. The agents and anchors are within a region of interest (ROI) given by $15\,\mathrm{m} \times 15\,\mathrm{m}$, where 25 anchors are deployed on a grid while 10 agents are uniformly randomly deployed within the ROI.[4] An example illustrating the anchor/agent layout is shown in Fig. 3.

[4]In order to exploit the spatial correlation features of QuaDRiGa, we deploy 10 agents in one instantiation of the simulation, where each agent runs the proposed algorithm independently.

TABLE I
LINK BUDGET FOR THE MMWAVE SYSTEM.

Quantity	Value
EIRP	10-30 dBm
Rx gain	2 dBi
Bandwidth	100 MHz
Noise figure	10 dB
Noise	-94 dBm
Noise PSD	-174 dBm/Hz

We assume that each agent has access to K nearest anchors. For each agent-anchor pair, the LOS probability is given by [59]

$$P_{\mathrm{LOS}} = \begin{cases} 1 & d \leqslant 1.2\,\mathrm{m} \\ e^{-\frac{d-1.2}{4.7}} & 1.2\,\mathrm{m} < d \leqslant 6.5\,\mathrm{m} \\ 0.32\, e^{-\frac{d-6.5}{32.6}} & d > 6.5\,\mathrm{m} \end{cases} \tag{26}$$

and the spatial correlation is implemented according to [71].

The link budget is chosen according to the FCC regulations and 3GPP standard [59], as shown in Table I. In addition, we adopt the free-space path loss model for the propagation between transmitters and receivers. The received signal-to-noise ratio (SNR) can be calculated based on link budget and node positions.

The input to our CIR-based localization algorithm is the estimated CIR values, which are emulated as follows. Given the node positions and LOS/NLOS conditions, QuaDRiGa generates the channel coefficients, which are transformed into CSI. The CSI measurements are then generated by adding zero-mean Gaussian noise according to the received SNR level. The noisy CSI is fed into the channel estimator, which produces the estimated CIR as the input to our algorithm [22]. The parameters are selected as $P_{\mathrm{NL}} = 0.1$, $P_{\mathrm{E}} = 0.1$, $\theta_{\max} = \frac{15}{c_0}$, and $\xi = 10^{8.42}$ according to the considered scenario and standard [59].

For the performance metric, the root mean square error (RMSE) of the inferred agent positions with respect to the true agent positions and its empirical cumulative distribution function (CDF) are considered.

B. Simulation Results

We first investigate the effect of the number of anchors K that each agent connects to on the localization performance. In particular, we fix the equivalent isotropically radiated power (EIRP) at 10 dBm, and plot the CDF of the resulting RMSE in Fig. 4. Note that, due to weak penetrating ability of mmWave signals, it is common to deploy anchors densely in indoor scenarios since there are walls and obstacles that may block the channel. As a result, a device may easily have access to 4, 5, or 6 nearby anchors. Table II shows the mean, 80th, and 90th percentile RMSE for 4, 5, and 6 anchors cases. We can see from the table that in most cases our algorithm achieves decimeter localization accuracy, and connecting to more neighboring anchors can significantly improve the localization performance.

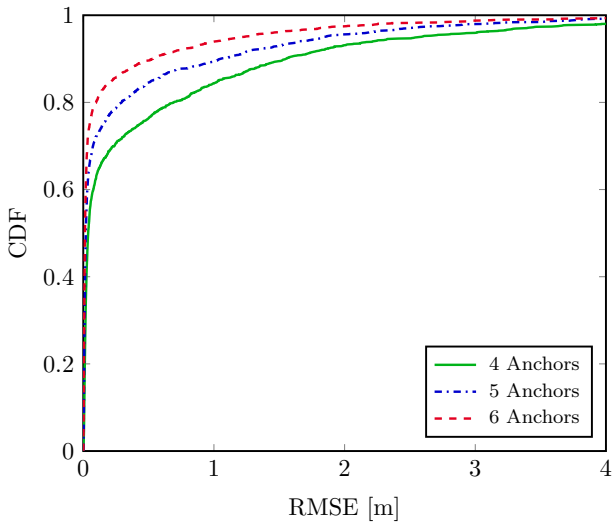

Fig. 4. Empirical CDF of RMSE for different number of connected anchors.

TABLE II
EFFECTS OF DIFFERENT NUMBER OF CONNECTED ANCHORS.

	Mean [m]	80th Perc. [m]	90th Perc. [m]
4 Anchors	0.48	0.69	1.56
5 Anchors	0.32	0.30	1.06
6 Anchors	0.21	0.10	0.54

We next investigate the effect of the EIRP on the localization performance when four anchors are connected to each agent. Fig. 5 shows how localization performance improves with larger EIRP since the SNR is increased. The mean, 80th, and 90th percentile RMSE for 10 dBm, 20 dBm, and 30 dBm EIRP cases are listed in Table III. We notice that compared with adding connected anchors, the performance gain by increasing EIRP is relatively small. This is due to the fact that with four connected anchors, for several simulation instantiations fewer than three agent-anchor pairs are in LOS condition, in which cases increasing EIRP benefits the localization accuracy only marginally compared to adding connected anchors.

VI. CONCLUSION

This paper developed a SI-based localization algorithm that exploits CIR estimates and thus is applicable to a variety of systems. In particular, we proposed a delay-origin uncertainty model describing the conditional distribution of the delays in CIR given node positions. Based on this model, we designed a localization algorithm utilizing a BP technique with the assistance of importance sampling, making the implementation efficient and scalable. Simulation results showed that our localization algorithm achieves decimeter-level localization accuracy in typical indoor environments using mmWave signals. It is also observed that, in the considered setting, a 50% increase in the number of anchors (from 4 to 6) is more beneficial than a two-order of magnitude increase in the emitted power (from 10 to 30 dBm). This is due to the fact that the improvement of LOS conditions is more crucial than the increasing of the received SNR.

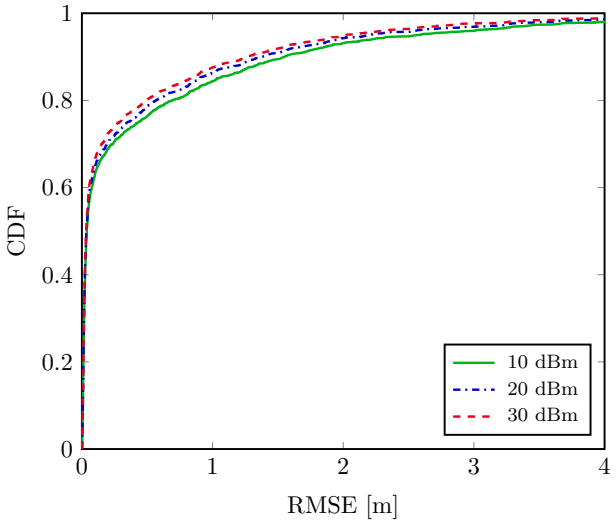

Fig. 5. Empirical CDF of RMSE for different EIRPs of the anchors.

TABLE III
EFFECTS OF DIFFERENT EIRPS OF THE ANCHORS.

	Mean [m]	80th Perc. [m]	90th Perc. [m]
10 dBm	0.48	0.69	1.56
20 dBm	0.42	0.57	1.38
30 dBm	0.38	0.50	1.27

REFERENCES

[1] M. Z. Win, A. Conti, S. Mazuelas, Y. Shen, W. M. Gifford, D. Dardari, and M. Chiani, "Network localization and navigation via cooperation," *IEEE Commun. Mag.*, vol. 49, no. 5, pp. 56–62, May 2011.

[2] A. T. Ihler, J. W. Fisher III, R. L. Moses, and A. S. Willsky, "Nonparametric belief propagation for self-localization of sensor networks," *IEEE J. Sel. Areas Commun.*, vol. 23, no. 4, pp. 809–819, Apr. 2005.

[3] M. Z. Win, Y. Shen, and W. Dai, "A theoretical foundation of network localization and navigation," *Proc. IEEE*, vol. 106, no. 7, pp. 1136–1165, Jul. 2018, special issue on *Foundations and Trends in Localization Technologies*.

[4] K. Pahlavan, X. Li, and J.-P. Mäkelä, "Indoor geolocation science and technology," *IEEE Commun. Mag.*, vol. 40, no. 2, pp. 112–118, Feb. 2002.

[5] N. Patwari, J. N. Ash, S. Kyperountas, A. O. Hero, R. L. Moses, and N. S. Correal, "Locating the nodes: Cooperative localization in wireless sensor networks," *IEEE Signal Process. Mag.*, vol. 22, no. 4, pp. 54–69, Jul. 2005.

[6] A. H. Sayed, A. Tarighat, and N. Khajehnouri, "Network-based wireless location: Challenges faced in developing techniques for accurate wireless location information," *IEEE Signal Process. Mag.*, vol. 22, no. 4, pp. 24–40, Jul. 2005.

[7] F. Zabini and A. Conti, "Inhomogeneous Poisson sampling of finite-energy signals with uncertainties in $\mathbb{R}^d$," *IEEE Trans. Signal Process.*, vol. 64, no. 18, pp. 4679–4694, Sep. 2016.

[8] R. Karlsson and F. Gustafsson, "The future of automotive localization algorithms: Available, reliable, and scalable localization: Anywhere and anytime," *IEEE Signal Process. Mag.*, vol. 34, no. 2, pp. 60–69, Mar. 2017.

[9] D. Dardari, A. Conti, C. Buratti, and R. Verdone, "Mathematical evaluation of environmental monitoring estimation error through energy-efficient wireless sensor networks," *IEEE Trans. Mobile Comput.*, vol. 6, no. 7, pp. 790–802, Jul. 2007.

[10] M. Z. Win, F. Meyer, Z. Liu, W. Dai, S. Bartoletti, and A. Conti, "Efficient multi-sensor localization for the Internet-of-Things," *IEEE Signal Process. Mag.*, vol. 35, no. 5, pp. 153–167, Sep. 2018.

[11] A. Sandryhaila and J. M. F. Moura, "Big data analysis with signal processing on graphs: Representation and processing of massive data sets with irregular structure," *IEEE Signal Process. Mag.*, vol. 31, no. 5, pp. 80–90, Sep. 2014.

[12] A. Conti, M. Guerra, D. Dardari, N. Decarli, and M. Z. Win, "Network experimentation for cooperative localization," *IEEE J. Sel. Areas Commun.*, vol. 30, no. 2, pp. 467–475, Feb. 2012.

[13] A. Conti, D. Dardari, M. Guerra, L. Mucchi, and M. Z. Win, "Experimental characterization of diversity navigation," *IEEE Syst. J.*, vol. 8, no. 1, pp. 115–124, Mar. 2014.

[14] U. A. Khan, S. Kar, and J. M. F. Moura, "Distributed sensor localization in random environments using minimal number of anchor nodes," *IEEE Trans. Signal Process.*, vol. 57, no. 5, pp. 2000–2016, May 2009.

[15] S. Safavi, U. A. Khan, S. Kar, and J. M. F. Moura, "Distributed localization: A linear theory," *Proc. IEEE*, vol. 106, no. 7, pp. 1204–1223, Jul. 2018.

[16] M. Z. Win, W. Dai, Y. Shen, G. Chrisikos, and H. V. Poor, "Network operation strategies for efficient localization and navigation," *Proc. IEEE*, vol. 106, no. 7, pp. 1224–1254, Jul. 2018, special issue on *Foundations and Trends in Localization Technologies*.

[17] T. Wang, Y. Shen, A. Conti, and M. Z. Win, "Network navigation with scheduling: Error evolution," *IEEE Trans. Inf. Theory*, vol. 63, no. 11, pp. 7509–7534, Nov. 2017.

[18] F. S. Cattivelli and A. H. Sayed, "Distributed nonlinear Kalman filtering with applications to wireless localization," in *Proc. IEEE Int. Conf. Acoustics, Speech, and Signal Process.*, Dallas, TX, USA, Mar. 2010, pp. 3522–3525.

[19] R. Abdolee, S. Saur, B. Champagne, and A. H. Sayed, "Diffusion LMS localization and tracking algorithm for wireless cellular networks," in *Proc. IEEE Int. Conf. Acoustics, Speech, and Signal Process.*, Vancouver, Canada, May 2013, pp. 4598–4602.

[20] P. S. Henry and H. Luo, "WiFi: What's next," *IEEE Commun. Mag.*, vol. 40, no. 12, pp. 66–72, Dec. 2002.

[21] Y. Xie, Z. Li, and M. Li, "Precise power delay profiling with commodity WiFi," *IEEE Trans. Mobile Comput.*, vol. 18, no. 6, pp. 1342–1355, 2018.

[22] Z. Yu, "Towards Location-Awareness in next generation wireless networks: A new approach based on channel state information," Master's thesis, Department of Aeronautics and Astronautics, Massachusetts Institute of Technology, Cambridge, MA, May 2020, thesis advisor: Professor Moe Z. Win.

[23] D. Vasisht, S. Kumar, and D. Katabi, "Decimeter-level localization with a single WiFi access point," in *Proc. of the USENIX Conf. on Networked Systems Design and Implementation*, Santa Clara, CA, Mar. 2016, pp. 165–178.

[24] K. Wu, J. Xiao, Y. Yi, M. Gao, and L. M. Ni, "FILA: Fine-grained indoor localization," in *Proc. IEEE Int. Conf. on Computer Commun.*, Orlando, FL, USA, 2012, pp. 2210–2218.

[25] X. Wang, L. Gao, and S. Mao, "BiLoc: Bi-modal deep learning for indoor localization with commodity 5GHz WiFi," *IEEE Access*, vol. 5, pp. 4209–4220, 2017.

[26] J. C. Haartsen, "The Bluetooth radio system," *IEEE Personal Commun. Mag.*, vol. 7, no. 1, pp. 28–36, 2000.

[27] P. Lazik, N. Rajagopal, O. Shih, B. Sinopoli, and A. Rowe, "ALPS: A Bluetooth and ultrasound platform for mapping and localization," in *Proc. ACM Conf. on Embedded Networked Sensor Systems*, Seoul, South Korea, Nov. 2015, pp. 73–84.

[28] Z. Liu, W. Dai, and M. Z. Win, "Mercury: An infrastructure-free system for network localization and navigation," *IEEE Trans. Mobile Comput.*, vol. 17, no. 5, pp. 1119–1133, May 2018.

[29] M. Altini, D. Brunelli, E. Farella, and L. Benini, "Bluetooth indoor localization with multiple neural networks," in *Proc. IEEE Int. Conf. on Pervasive Comput. and Commun.*, 2010, pp. 295–300.

[30] M. Z. Win and R. A. Scholtz, "Impulse radio: How it works," *IEEE Commun. Lett.*, vol. 2, no. 2, pp. 36–38, Feb. 1998.

[31] M. Z. Win, "Spectral density of random UWB signals," *IEEE Commun. Lett.*, vol. 6, no. 12, pp. 526–528, Dec. 2002.

[32] M. Z. Win and R. A. Scholtz, "Ultra-wide bandwidth time-hopping spread-spectrum impulse radio for wireless multiple-access communications," *IEEE Trans. Commun.*, vol. 48, no. 4, pp. 679–691, Apr. 2000.

[33] D. Dardari, A. Conti, J. Lien, and M. Z. Win, "The effect of cooperation on localization systems using UWB experimental data," *EURASIP J. Appl. Signal Process.*, vol. 2008, pp. 1–11, Article ID 513 873, 2008, special issue on *Cooperative Localization in Wireless Ad Hoc and Sensor Networks*.

[34] H. Wymeersch, S. Maranò, W. M. Gifford, and M. Z. Win, "A machine learning approach to ranging error mitigation for UWB localization," *IEEE Trans. Commun.*, vol. 60, no. 6, pp. 1719–1728, Jun. 2012.

[35] D. Dardari, A. Conti, U. J. Ferner, A. Giorgetti, and M. Z. Win, "Ranging with ultrawide bandwidth signals in multipath environments," *Proc. IEEE*, vol. 97, no. 2, pp. 404–426, Feb. 2009, special issue on *Ultra-Wide Bandwidth (UWB) Technology & Emerging Applications*.

[36] S. Gezici, Z. Tian, G. B. Giannakis, H. Kobayashi, A. F. Molisch, H. V. Poor, and Z. Sahinoglu, "Localization via ultra-wideband radios: A look at positioning aspects for future sensor networks," *IEEE Signal Process. Mag.*, vol. 22, no. 4, pp. 70–84, Jul. 2005.

[37] S. Gezici and H. V. Poor, "Position estimation via ultra-wide-band signals," *Proc. IEEE*, vol. 97, no. 2, pp. 386–403, Feb. 2009.

[38] B. Teague, Z. Liu, F. Meyer, and M. Z. Win, "Peregrine: 3-D network localization and navigation," in *Proc. IEEE Latin-American Conf. Commun.*, Guatemala City, Guatemala, Nov. 2017, pp. 1–6.

[39] S. Rangan, T. S. Rappaport, and E. Erkip, "Millimeter-wave cellular wireless networks: Potentials and challenges," *Proc. IEEE*, vol. 102, no. 3, pp. 366–385, 2014.

[40] H. Deng and A. Sayeed, "Mm-Wave MIMO channel modeling and user localization using sparse beamspace signatures," in *Proc. IEEE Workshop on Signal Process. Advances in Wireless Commun.*, Toronto, Canada, 2014, pp. 130–134.

[41] F. Lemic, J. Martin, C. Yarp, D. Chan, V. Handziski, R. Brodersen, G. Fettweis, A. Wolisz, and J. Wawrzynek, "Localization as a feature of mmWave communication," in *Proc. Int. Wireless Commun. and Mobile Comput.*, Paphos, Cyprus, 2016, pp. 1033–1038.

[42] R. Mendrzik, F. Meyer, G. Bauch, and M. Z. Win, "Enabling situational awareness in millimeter wave massive MIMO systems," *IEEE J. Sel. Topics Signal Process.*, vol. 13, no. 5, pp. 1196–1211, Sep. 2019.

[43] A. H. Kemp and E. B. Bryant, "CIR measurement system for characterisation of wideband communication channels in the 2.4 GHz ISM band," *Journal of Electrical Engineering*, vol. 57, no. 3, pp. 146–153, 2006.

[44] S. Maranò, W. M. Gifford, H. Wymeersch, and M. Z. Win, "NLOS identification and mitigation for localization based on UWB experimental data," *IEEE J. Sel. Areas Commun.*, vol. 28, no. 7, pp. 1026–1035, Sep. 2010.

[45] I. Guvenc, C.-C. Chong, and F. Watanabe, "NLOS identification and mitigation for UWB localization systems," in *Proc. IEEE Wireless Commun. and Networking Conf.*, Kowloon, Hong Kong, Mar. 2007, pp. 1571–1576.

[46] S. Bartoletti, A. Giorgetti, M. Z. Win, and A. Conti, "Blind selection of representative observations for sensor radar networks," *IEEE Trans. Veh. Technol.*, vol. 64, no. 4, pp. 1388–1400, Apr. 2015.

[47] I. Güvenç, C.-C. Chong, F. Watanabe, and H. Inamura, "NLOS identification and weighted least-squares localization for UWB systems using multipath channel statistics," *EURASIP J. Adv. in Signal Process.*, vol. 2008, pp. 1–14, Article ID 271 984, 2008.

[48] A. Conti, S. Mazuelas, S. Bartoletti, W. C. Lindsey, and M. Z. Win, "Soft information for localization-of-things," *Proc. IEEE*, vol. 107, no. 11, pp. 2240–2264, Nov. 2019.

[49] S. Mazuelas, A. Conti, J. C. Allen, and M. Z. Win, "Soft range information for network localization," *IEEE Trans. Signal Process.*, vol. 66, no. 12, pp. 3155–3168, Jun. 2018.

[50] S. Bartoletti, W. Dai, A. Conti, and M. Z. Win, "A mathematical model for wideband ranging," *IEEE J. Sel. Topics Signal Process.*, vol. 9, no. 2, pp. 216–228, Mar. 2015.

[51] S. Bartoletti, W. Dai, A. Conti, and M. Z. Win, "Wideband localization via range likelihood based on reduced dataset," in *Proc. IEEE Canadian Workshop on Inf. Theory*, St. John's, NL, Canada, Jul. 2015, pp. 93–96.

[52] S. Jaeckel, L. Raschkowski, K. Börner, and L. Thiele, "QuaDRiGa: A 3-D multi-cell channel model with time evolution for enabling virtual field trials," *IEEE Trans. Antennas Propag.*, vol. 62, no. 6, pp. 3242–3256, Jun. 2014.

[53] D. Shutin, W. Wang, and T. Jost, "Incremental sparse Bayesian learning for parameter estimation of superimposed signals," in *Proc. Intl. Conf. on Sampling Theory and Applications*, Bremen, Germany, Jul. 2013, pp. 6–9.

[54] M.-A. Badiu, T. L. Hansen, and B. H. Fleury, "Variational Bayesian inference of line spectra," *IEEE Trans. Signal Process.*, vol. 65, no. 9, pp. 2247–2261, 2017.

[55] Y. Shen and M. Z. Win, "Fundamental limits of wideband localization – Part I: A general framework," *IEEE Trans. Inf. Theory*, vol. 56, no. 10, pp. 4956–4980, Oct. 2010.

[56] J. L. Williams and R. Lau, "Approximate evaluation of marginal association probabilities with belief propagation," *IEEE Trans. Aerosp. Electron. Syst.*, vol. 50, no. 4, pp. 2942–2959, Oct. 2014.

[57] F. Meyer, T. Kropfreiter, J. L. Williams, R. A. Lau, F. Hlawatsch, P. Braca, and M. Z. Win, "Message passing algorithms for scalable multitarget tracking," *Proc. IEEE*, vol. 106, no. 2, pp. 221–259, Feb. 2018.

[58] J. L. Williams and R. A. Lau, "Multiple scan data association by convex variational inference," *IEEE Trans. Signal Process.*, vol. 66, no. 8, pp. 2112–2127, Apr. 2018.

[59] *Study on Channel Model for Frequencies from 0.5 to 100 GHz*, 3rd Generation Partnership Project 3GPP™ TR 38.901 V15.0.0 (2018-06), Jun. 2018, release 15.

[60] J. Winn and C. M. Bishop, "Variational message passing," *Journal of Machine Learning Research*, vol. 6, pp. 661–694, 2005.

[61] D. Koller and N. Friedman, *Probabilistic Graphical Models: Principles and Techniques*. Cambridge, MA: MIT Press, 2009.

[62] H.-A. Loeliger, "An introduction to factor graphs," *IEEE Signal Process. Mag.*, vol. 21, no. 1, pp. 28–41, 2004.

[63] F. R. Kschischang, B. J. Frey, and H.-A. Loeliger, "Factor graphs and the sum-product algorithm," *IEEE Trans. Inf. Theory*, vol. 47, no. 2, pp. 498–519, Feb. 2001.

[64] T. Heskes, "Stable fixed points of loopy belief propagation are local minima of the Bethe free energy," in *Proc. Advances in Neural Inform. Process. Systems*, British Columbia, Canada, Dec. 2002, pp. 359–366.

[65] J. Yedidia, W. Freeman, and Y. Weiss, "Understanding belief propagation and its generalizations," *Exploring Artificial Intelligence in the new millennium*, vol. 8, pp. 236–239, 2003.

[66] J. Yedidia, W. Freeman, and Y. Weiss, "Constructing free-energy approximations and generalized belief propagation algorithms," *IEEE Trans. Inf. Theory*, vol. 51, no. 7, pp. 2282–2312, July 2005.

[67] R. Y. Rubinstein and D. P. Kroese, *Simulation and the Monte Carlo Method*. New York, NY: John Wiley & Sons, 2016, vol. 10.

[68] D. P. Kroese, T. Taimre, and Z. I. Botev, *Handbook of Monte Carlo methods*. John Wiley & Sons, 2013, vol. 706.

[69] C. P. Robert and G. Casella, *Monte Carlo Statistical Methods* . Springer, 2005.

[70] J. Lee, E. Tejedor, K. Ranta-aho, H. Wang, K.-T. Lee, E. Semaan, E. Mohyeldin, J. Song, C. Bergljung, and S. Jung, "Spectrum for 5G: Global status, challenges, and enabling technologies," *IEEE Commun. Mag.*, vol. 56, no. 3, pp. 12–18, 2018.

[71] F. Ademaj, M. K. Müller, S. Schwarz, and M. Rupp, "Modeling of spatially correlated geometry-based stochastic channels," in *Proc. IEEE Semiannual Veh. Technol. Conf.*, Toronto, Canada, Sep. 2017.